

Invited talk at the 15th Int. Conf. on Few-Body Problems in Physics
 Groningen, The Netherlands, 22-26 July, 1997
 ADP-97-32/T265, DOE/ER/40762-129, UM PP 98-016

Deuteron Structure Functions in the Context of Few-Body Physics

A. W. Thomas^a and W. Melnitchouk^b

^aDepartment of Physics and Mathematical Physics,
 and Special Research Centre for the Subatomic Structure of Matter,
 University of Adelaide, Adelaide, Australia 5005

^bDepartment of Physics, University of Maryland,
 College Park, Maryland 20742, USA

Few-body systems offer a unique challenge to those interested in deep-inelastic scattering. Using the deuteron as the simplest and most easily solvable nuclear system we review the main physics issues in the valence and sea quark regimes. For the former the key issue is the understanding of Fermi motion and binding corrections, and our ability to extract the ratio F_2^n/F_2^p as $x \rightarrow 1$. The most recent analysis of deuteron data for F_2^n/F_2^p is consistent with perturbative QCD, but inconsistent with the assumptions common to all standard parton distribution fits. This should be taken into account in calculating event rates at HERA — especially at large x and Q^2 . The extraction of g_1^n also presents an opportunity to refine the description of nuclear effects in spin-dependent structure functions. In the region of small x one must correct for shadowing and meson exchange current effects to explore the flavor structure of sea, which is, in turn, deeply related to the chiral structure of the nucleon.

1. INTRODUCTION

The study of nuclear deep-inelastic scattering, particularly on the deuteron, began in the 1970's, primarily as a source of information on the neutron structure function. There was an explosion of interest in the subject following the announcement of the nuclear EMC effect in 1983 [1]. For an introduction to the ideas of deep-inelastic scattering and to the nuclear EMC effect we refer to recent reviews [2,3]. While the question of how the structure of the nucleon is modified in medium [4] and how that may be investigated using deep-inelastic scattering (DIS) [5] is both timely and important, it is not our prime concern here. Instead, we concentrate on the deuteron as a source of information about the structure of the neutron and as a laboratory for testing our understanding of nuclear corrections such as binding, Fermi motion, shadowing and meson exchange currents (MEC). If we cannot understand these phenomena in a system as weakly bound as the deuteron, then we shall certainly not understand them in any heavier system.

In section 2 we briefly review the history of binding and Fermi motion corrections, leading to a simple one-dimensional convolution of the nucleon momentum distribution

with the free nucleon structure function. Recent work on the off-shell corrections to such a treatment is then summarized, before we turn to a very interesting physics question, namely the validity, or otherwise, of the perturbative QCD (PQCD) predictions for the asymptotic d/u ratio in the proton. This issue also seems to have consequences for the analysis of the anomaly at large x and Q^2 recently observed by ZEUS and H1 at HERA. The extension to the spin dependent structure function of the neutron, g_1^n , is also outlined.

In section 3 we turn to nuclear corrections at small x , the region dominated by sea quarks. The major surprise in this region in recent years was the discovery of a significant violation of the Gottfried sum rule [6], which implied a major difference in the number of \bar{u} and \bar{d} quarks in the proton — a conclusion supported in graphic fashion by recent Drell-Yan data from Fermilab experiment E866 [7]. The origin of this asymmetry seems to be the pion cloud of the nucleon [8,9], which is a non-perturbative consequence of dynamical chiral symmetry breaking and which cannot be avoided *even* in the deep-inelastic regime.

2. THE DEUTERON AT LARGE x

The early work on DIS from the deuteron was aimed primarily at extracting the neutron structure function [10–12]. Amongst the many approaches to this problem we mention the light-front treatment [13,14] and the relativistic impulse approximation [15,16], involving the free nucleon structure function at a shifted value of x or Q^2 [17,18]. A more phenomenological approach, developed by Frankfurt and Strikman [19], attempts to derive the nuclear correction in the deuteron by extrapolation from higher A as a function of the “effective density” of the nucleus. The experimental extraction of F_2^n is usually made using either the phenomenological effective density approach or the older, “pre-EMC” theoretical treatments. We shall see that in particular the latter are not satisfactory, and that taking into account the main lessons of the EMC effect leads to a surprisingly large change in the conclusions concerning the ratio F_2^n/F_2^p in the region $x \rightarrow 1$.

The traditional impulse approximation treatment of the deuteron structure function assumes a convolution of the free nucleon structure function, F_2^N , with the non-relativistic momentum distribution $f_{N/D}$ of nucleons in the deuteron, calculated in terms of a non-relativistic wave function of the deuteron and its binding energy. Although the binding energy is very small, the kinetic energy of the recoiling nucleon plays a significant role in forcing the struck nucleon further off-shell than one would usually expect — as first pointed out by Dunne and Thomas [17]:

$$f_{N/D}(y) \sim y \int d^3p |\psi_D(\vec{p})|^2 \delta\left(y - \frac{M_D - M - \vec{p}^2/2M}{M}\right), \quad (1)$$

where p is the off-shell nucleon momentum, y is the light-cone nucleon momentum fraction, and ψ_D is the deuteron wave function. Note that the “flux-factor”, y , was omitted in early work, but as noted by many authors [19,20] it is important in practice.

2.1. Covariant Formulation

In order to assess the theoretical reliability of the non-relativistic impulse approximation one needs to go beyond the usual assumptions made in the convolution approach [21]. In particular, the ingredients necessary for a covariant, relativistic description are a covariant

DNN vertex with one of the nucleons (the spectator to the hard collision) on-mass-shell, and an off-shell photon–nucleon scattering amplitude (“off-shell nucleon structure function”) \widehat{W} , the full structure of which was only recently derived in Ref.[22].

The covariant DNN vertex was written down many years ago by Blankenbecler and Cook [23] and, at least in the rest frame of the deuteron, can be expressed in terms of relativistic deuteron wave functions [24,25]. The deuteron structure function can then be written in terms of the Dirac trace of the product $(A_0 + \gamma^\mu A_{1\mu})\widehat{W}$, where the combination $(A_0 + \gamma^\mu A_{1\mu})$ includes all of the information on the deuteron vertex and (on-mass-shell) spectator nucleon, summed over spin projections and can be calculated in terms of the relativistic deuteron wave function.

The analysis of Ref.[22] showed that the most general form of the operator \widehat{W} (which is a 4×4 matrix in Dirac space), consistent with the discrete symmetries and gauge invariance, which contributes in the Bjorken limit is:

$$\widehat{W} = \widehat{W}_0 I + \widehat{W}_1 \not{p} + \widehat{W}_2 \not{q}, \quad (2)$$

where the \widehat{W}_i are functions of p^2, q^2 and $p \cdot q$ (q is the virtual photon four-momentum). Thus, whereas in the free case the nucleon structure function involves the combination:

$$\text{Tr}[(\not{p} + M)\widehat{W}] \sim M\widehat{W}_0 + M^2\widehat{W}_1 + p \cdot q \widehat{W}_2, \quad (3)$$

the deuteron structure function involves:

$$\text{Tr}[(A_0 + \gamma^\mu A_{1\mu})\widehat{W}] \sim A_0\widehat{W}_0 + p \cdot A_1\widehat{W}_1 + q \cdot A_1\widehat{W}_2. \quad (4)$$

Clearly then, even in the absence of Fermi motion one finds that in general:

$$F_2^D \neq F_2^N, \quad (5)$$

unless, as is usually implicitly assumed [21], only one of the \widehat{W}_i is non-zero [22].

Having established that, in principle, the structure function of the bound nucleon cannot equal the structure function of the free nucleon, the important question is how big the difference actually is in practice. To estimate this, one can construct a simple model [22] of the so-called hand-bag diagram for an off-shell nucleon, in which the N -quark vertex is taken to be either a simple scalar or pseudo-vector, with the parameters adjusted to reproduce the free nucleon structure functions [26]. It is then possible to manipulate the exact deuteron structure function into the form [27]:

$$F_2^D = F_2^{D(\text{conv})} + \delta^{(\text{off})} F_2^D, \quad (6)$$

where the convolution component:

$$F_2^{D(\text{conv})}(x, Q^2) = \frac{1}{2} \sum_N \int_x^{M_D/M} dy \phi_{N/D}(y) F_2^N\left(\frac{x}{y}, Q^2\right), \quad (7)$$

now involves the relativistic momentum distribution of nucleons in the deuteron [27] (i.e. $\phi_{N/D}(y)$ depends on all components of the relativistic deuteron wave function, $u^2 + w^2 + v_s^2 + v_t^2$ [24]). Note that the argument of the free nucleon structure function F_2^N indicates that we need to find a quark with momentum x in a nucleon with momentum y .

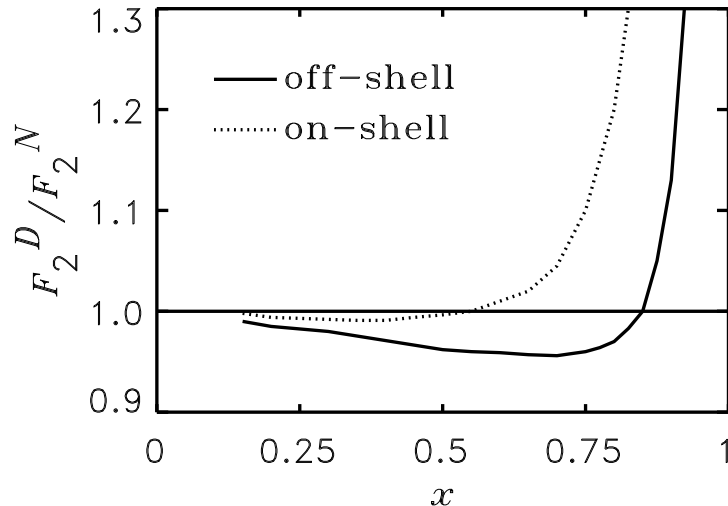


Figure 1. F_2^D/F_2^N ratio as a function of x for the model of Refs.[22,27] (solid) which accounts for off-shell kinematics, and the on-shell model of Ref.[13] (dotted) — from Ref.[27].

Furthermore, the “non-convolution” correction term $\delta^{(\text{off})}F_2^D$ can be separated into two pieces associated with off-mass-shell corrections at the DN and γ^*N vertices [27].

The result of the fully off-shell calculation from Ref.[27] is shown in Fig.1 (solid curve), where the ratio of the total deuteron to nucleon structure functions (F_2^D/F_2^N) is plotted. We also show the result of an on-mass-shell calculation from Ref.[13] (dotted curve), which has been used in many previous analyses of the deuteron data [1,28]. The most striking difference between the curves is the fact that the on-shell ratio has a very much smaller trough at $x \approx 0.3$, and rises faster above unity (at $x \approx 0.5$) than the off-shell curve, which has a deeper trough, at $x \approx 0.6 - 0.7$, and rises above unity somewhat later (at $x \approx 0.8$).

The behaviour of the full off-shell curve in Fig.1 is qualitatively similar to that found by Uchiyama and Saito [29], Kaptari and Umnikov [14], and Braun and Tokarev [16], who also used off-mass-shell kinematics. However, these authors did not include the (small) non-convolution correction term, $\delta^{(\text{off})}F_2^D$. The on-shell calculation [13], on the other hand, was performed in the infinite momentum frame where the nucleons are on-mass-shell. The problem with this approach in the past has been the lack of reliable deuteron wave functions in the infinite momentum frame, and only recently have the first steps been taken in calculating deuteron wave functions on the light-cone [30]. In practice one has usually made use of the non-relativistic, S - and D -state deuteron wave functions calculated in the deuteron rest frame, without accounting for the explicit binding effects which should show up in the infinite momentum frame in the form of additional Fock

components (e.g., NN -meson(s)) in the nuclear wave function.

Clearly, a smaller D/N ratio at large x , as in Refs.[22,27], implies a larger neutron structure function in this region. To estimate the size of the effect on the n/p ratio requires one to “deconvolute” Eq.(7) in order to extract F_2^n . To study nuclear effects on the neutron structure function arising from different models of the deuteron, one must eliminate any effects that may arise from the extraction method itself. Melnitchouk and Thomas [31] therefore use exactly the same extraction procedure as used in previous EMC [1] and SLAC [28] data analyses, namely the smearing (or deconvolution) method discussed by Bodek *et al.* [32]. *This method involves the direct use of the proton and deuteron data, without making any assumption concerning F_2^n itself.* For completeness we briefly outline the main ingredients in this method.

Firstly, one subtracts from the deuteron data, F_2^D , the additive, off-shell corrections, $\delta^{(\text{off})} F_2^D$, to give the convolution part, $F_2^{D(\text{conv})}$. Then one smears the proton data, F_2^p , with the nucleon momentum distribution function $\phi_{N/D}(y)$ in Eq.(7) to give $\tilde{F}_2^p \equiv F_2^p/S_p$. The smeared neutron structure function, \tilde{F}_2^n , is then obtained from:

$$\tilde{F}_2^n = F_2^{D(\text{conv})} - \tilde{F}_2^p. \quad (8)$$

Since the smeared neutron structure function is defined as $\tilde{F}_2^n \equiv F_2^n/S_n$, we can invert this to obtain the structure function of a free neutron:

$$F_2^n = S_n \left(F_2^{D(\text{conv})} - F_2^p/S_p \right). \quad (9)$$

In Eq.(9), the proton smearing factor, S_p , can be computed at each x from the function $\phi_{N/D}(y)$, and a parameterization of the F_2^p data [33]. The neutron structure function may then be derived iteratively from Eq.(9). Taking as a first guess $S_n = S_p$, the values of F_2^n are smeared by the function $\phi_{N/D}(y)$, and the results used to obtain a better estimate for S_n . The new value for S_n is then used in Eq.(9) to obtain an improved estimate for F_2^n , and the procedure repeated until convergence is achieved.

The results of this procedure are presented in Fig.2, for both the off-shell calculation [27] (solid) and the on-shell model [13] (dotted). The increase in the off-shell ratio at large x is a direct consequence of the deeper trough in the F_2^D/F_2^N ratio in Fig.1. To illustrate the role of the non-convolution correction, $\delta^{(\text{off})} F_2^D$, we have also performed the analysis setting this term to zero, and approximating F_2^D by $F_2^{D(\text{conv})}(x)$. The effect of this correction (dashed curve in Fig.2) appears minimal. One can therefore attribute most of the difference between our analysis and the earlier, “pre-EMC”, on-shell results to kinematics — since both calculations involve essentially the same deuteron wave functions.

2.2. A Test of Perturbative QCD

The precise mechanism whereby the SU(6), spin-flavor symmetry of the parton distributions of the nucleon is broken is a question of fundamental importance in hadronic physics. In a world of exact SU(6) symmetry, the wave function of a proton, polarized say in the $+z$ direction, has the form [34]:

$$\begin{aligned} |p \uparrow\rangle &= \frac{1}{\sqrt{2}} |u \uparrow (ud)_{S=0}\rangle + \frac{1}{\sqrt{18}} |u \uparrow (ud)_{S=1}\rangle - \frac{1}{3} |u \downarrow (ud)_{S=1}\rangle \\ &\quad - \frac{1}{3} |d \uparrow (uu)_{S=1}\rangle - \frac{\sqrt{2}}{3} |d \downarrow (uu)_{S=1}\rangle, \end{aligned} \quad (10)$$

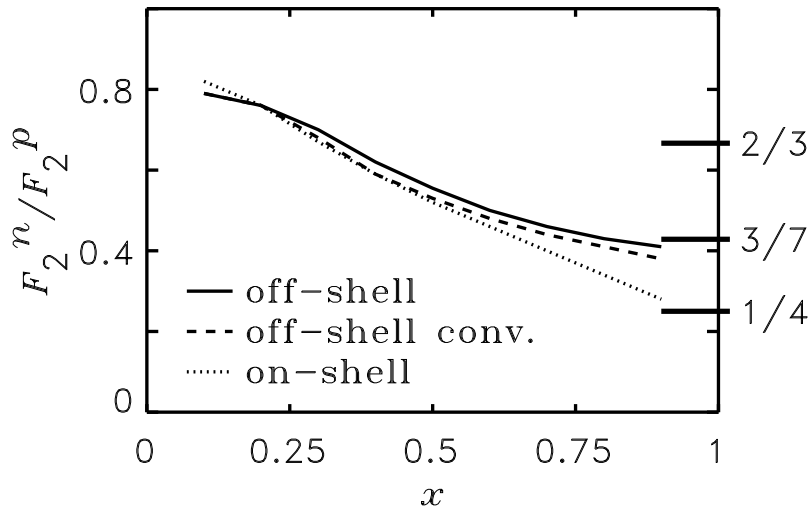


Figure 2. The ratio F_2^n/F_2^p as a function of x , for the off-shell model (solid), off-shell model without the convolution-breaking term (dashed), and the on-shell model (dotted). On the right-hand axis we have marked the $x \rightarrow 1$ limits of the SU(6) symmetric model (2/3), and the predictions of the models of Refs.[35,36] (1/4) and [38,39] (3/7).

where the subscript S denotes the total spin of the two-quark component. In this limit, the nucleon and Δ isobar would be degenerate. In deep-inelastic scattering, exact SU(6) symmetry would be manifested in equivalent shapes for the valence quark distributions of the proton, which would be related simply by $u_V(x) = 2d_V(x)$ for all x . For the neutron to proton structure function ratio this would imply:

$$\frac{F_2^n}{F_2^p} = \frac{2}{3} \quad ; \quad \text{SU(6) symmetry.} \quad (11)$$

Of course, Nature does not respect exact SU(6) spin-flavor symmetry. The nucleon and Δ masses are split by some 300 MeV, and empirically the d quark distribution is softer than the u . The correlation between the mass splitting in the **56** baryons and the large- x behavior of F_2^n/F_2^p was observed some time ago by Close [35] and Carlitz [36]. Based on phenomenological [35] and Regge [36] arguments, the breaking of the symmetry in Eq.(10) was argued to arise from a suppression of the “diquark” configurations having $S = 1$ relative to the $S = 0$ configuration. Such a suppression is, in fact, quite natural if one observes that whatever mechanism leads to the observed $N - \Delta$ splitting (e.g. color-magnetic force, instanton-induced interaction, pion exchange), necessarily acts to produce a mass splitting between the possible spin states of the spectator pair, $(qq)_S$, with the $S = 1$ state heavier than the $S = 0$ state by some 200 MeV [37]. From Eq.(10), a dominant scalar valence diquark component of the proton suggests that in the $x \rightarrow 1$

limit F_2^p is essentially given by a single quark distribution (i.e. the u), in which case:

$$\frac{F_2^n}{F_2^p} \rightarrow \frac{1}{4}, \quad \frac{d}{u} \rightarrow 0 \quad ; \quad S = 0 \text{ dominance.} \quad (12)$$

This expectation has, in fact, been built into all phenomenological fits to the parton distribution data.

An alternative suggestion, based on perturbative QCD, was originally formulated by Farrar and Jackson [38]. There it was argued that the exchange of longitudinal gluons, which are the only type permitted when the spin projections of the two quarks in $(qq)_S$ are aligned, would introduce a factor $(1-x)^{1/2}$ into the Compton amplitude — in comparison with the exchange of a transverse gluon between quarks with spins anti-aligned. In this approach the relevant component of the proton valence wave function at large x is that associated with states in which the total “diquark” spin *projection*, S_z , is zero. Consequently, scattering from a quark polarized in the opposite direction to the proton polarization is suppressed by a factor $(1-x)$ relative to the helicity-aligned configuration.

A similar result is also obtained in the treatment of Brodsky *et al.* [39] (based on counting-rules), where the large- x behavior of the parton distribution for a quark polarized parallel ($\Delta S_z = 1$) or antiparallel ($\Delta S_z = 0$) to the proton helicity is given by: $q^{\uparrow\downarrow}(x) = (1-x)^{2n-1+\Delta S_z}$, where n is the minimum number of non-interacting quarks (equal to 2 for the valence quark distributions). In the $x \rightarrow 1$ limit these arguments, based on PQCD, suggest:

$$\frac{F_2^n}{F_2^p} \rightarrow \frac{3}{7}, \quad \frac{d}{u} \rightarrow \frac{1}{5} \quad ; \quad S_z = 0 \text{ dominance.} \quad (13)$$

Note that the d/u ratio *does not vanish* in this case. Clearly, if one is to understand the dynamics of the nucleon’s quark distributions at large x , it is imperative that the consequences of these models be tested experimentally.

As explained above, our analysis of the SLAC data points [28,40] involves no assumption whatsoever about F_2^n , the only input is the nucleon momentum density in the deuteron, $\phi_{N/D}(y)$. The results of this reanalysis are shown in Fig.3, at an average value of $Q^2 \approx 12$ GeV². The data represented by the open circles have been extracted with the on-shell deuteron model of Ref.[13], while the filled circles were obtained using the off-shell model of Refs.[22,27]. Most importantly, the F_2^n/F_2^p points obtained with the off-shell method appear to approach a value broadly consistent with the Farrar-Jackson [38] prediction of 3/7, whereas the data previously analyzed in terms of the on-shell formalism produced a ratio tending to the lower value of 1/4.

The d/u ratio, shown in Fig.4, is obtained by inverting F_2^n/F_2^p in the valence quark dominated region. The points extracted using the off-shell formalism (solid circles) are again significantly above those obtained previously with the aid of the on-shell prescription. In particular, they indicate that the d/u ratio may actually approach a *finite* value in the $x \rightarrow 1$ limit, contrary to the expectation of the model of Refs.[35,36], in which d/u tends to zero. Although it is *a priori* not clear at which scale these model predictions should be valid, for the values of Q^2 corresponding to the analyzed data the effects of Q^2 evolution are minimal.

Naturally, it would be preferable to extract F_2^n at large x without having to deal with uncertainties in the nuclear effects. In principle this could be achieved by using neutrino

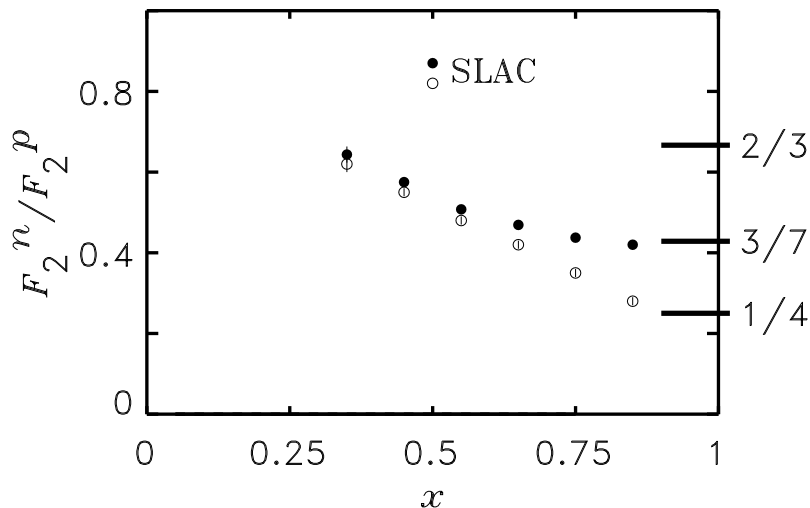


Figure 3. Deconvoluted F_2^n/F_2^p ratio extracted from the SLAC p and D data [28,40] using the model of Ref.[22,27] (solid circles) and Ref.[13] (open circles).

and antineutrino beams to measure the u and d distributions in the proton separately, and reconstructing F_2^n from these. Unfortunately, as seen in Fig.4, the neutrino data from the CDHS collaboration [41] do not extend out to very large x ($x > 0.6$), and at present cannot discriminate between the different methods of analyzing the electron–deuteron data.

2.3. Relevance of the d/u Ratio to the HERA Anomaly

The H1 and ZEUS experiments at HERA have recently produced a small number of events at enormously high Q^2 which have generated tremendous theoretical interest [42,43]. For $Q^2 > 10,000\text{GeV}^2$ and $x > 0.45$ the valence parton distributions are calculated to drop dramatically. The HERA anomaly is essentially the excess of observed “neutral current” events (i.e., events of the type $e^+p \rightarrow e^+X$) over expectations by roughly an order of magnitude. Many exotic explanations of this excess have already been suggested, indeed, the number of possibilities currently exceeds the number of events. However, before the new physics can be worked out one must be sure that the input parton distributions used to estimate “background” rates are reliable.

One glaring problem with the current treatment of the partonic “background” is that *all* of the standard distributions used are constructed to satisfy $d/u \rightarrow 0$ as $x \rightarrow 1$ at low- Q^2 . As we have seen, the recent re-analysis of the deuteron data leads to a d/u ratio which appears to be consistent with the prediction of PQCD that $d/u \rightarrow 1/5$ as $x \rightarrow 1$. In the light of this result it is not only vital to find alternative, more direct measurements of d/u at large x , but those generating standard sets of parton distributions should at the very

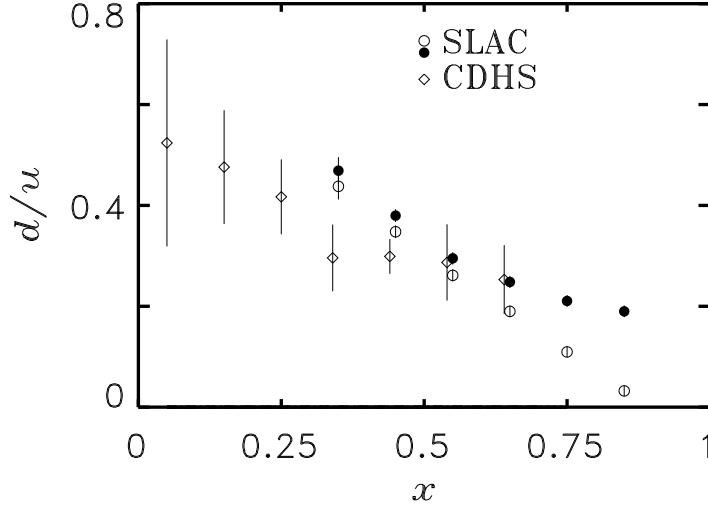


Figure 4. Extracted d/u ratio (see Fig.2). Also shown for comparison is the ratio extracted from neutrino measurements by the CDHS collaboration [41].

least present alternative parameter sets consistent with the new analysis of the deuteron data. Until parameter sets are constructed which are consistent with $d/u \rightarrow 1/5$ as $x \rightarrow 1$, at $Q^2 \sim 10 \text{ GeV}^2$, one cannot be sure of the reliability of “background” rate estimates at the extreme values of Q^2 and x being probed at HERA. Certainly one cannot hope to probe other exciting aspects of hadron structure, such as intrinsic charm and beauty [44–46], until the d/u issue has been resolved.

2.4. Spin Dependent Structure Functions

The spin structure functions of the nucleon, $g_1^{p(n)}$, are of tremendous interest at present. Experimentally, g_1 is proportional to the difference of DIS cross sections for ep scattering with beam and target helicities aligned and anti-aligned [47]. Within the parton model it may be written in terms of the parton helicity (loosely “spin”) distributions, $\Delta q(x) = [q^\uparrow - q^\downarrow + \bar{q}^\uparrow - \bar{q}^\downarrow]$, with $q^{\uparrow(\downarrow)}$ the number density of quarks with helicity parallel (anti-parallel) to the helicity of the target proton:

$$g_1^p(x) = \frac{1}{2} \sum_q e_q^2 \Delta q(x). \quad (14)$$

Intense interest in the spin structure functions began in 1988 when EMC announced a large violation of the Ellis-Jaffe sum rule [48], which relates $\Gamma_p(Q^2) \equiv \int_0^1 g_1^p(x, Q^2) dx$ to the isovector and octet axial-vector coupling constants, $g_A^{(3)}$ and $g_A^{(8)}$. The failure of this sum rule, which is not a rigorous consequence of QCD, led to questions about the Bjorken sum rule, which relates $\Gamma_p - \Gamma_n$ to $g_A^{(3)}/6$ (modulo QCD radiative corrections [49]) and *is*

a strict consequence of QCD. To determine Γ_n one must measure $g_1^n(x)$, which requires a polarized nuclear target such as ^3He or D . At present, all neutron data extracted from the deuteron are obtained by applying a simple, non-relativistic prescription to correct g_1^D for the D -state component (probability ω_D) of the deuteron wave function [50]:

$$g_1^n(x) = \left(1 - \frac{3}{2}\omega_D\right)^{-1} g_1^D(x) - g_1^p(x). \quad (15)$$

As we explain below, exactly the same techniques as described in the previous section may be used to test the accuracy of Eq.(15).

While most interest has been focussed on the issue of sum rules, we stress that the shapes of $g_1^p(x)$ and $g_1^n(x)$ contain even more important information. For example, the same arguments that led to different conclusions about the behaviour of d/u as $x \rightarrow 1$ also give quite different predictions for g_1^p and g_1^n as $x \rightarrow 1$, namely $1/4$ and $3/7$, respectively. Quite interestingly, while the ratio of the polarized to unpolarized u quark distributions is predicted to be the same in the two models:

$$\frac{\Delta u}{u} \rightarrow 1 \quad ; \quad S = 0 \text{ or } S_z = 0 \text{ dominance}, \quad (16)$$

the results for the d -quark distribution ratio differ even in sign:

$$\frac{\Delta d}{d} \rightarrow -\frac{1}{3} \quad ; \quad S = 0 \text{ dominance}, \quad (17)$$

$$\rightarrow 1 \quad ; \quad S_z = 0 \text{ dominance}. \quad (18)$$

Using the same techniques described in section 2.1 for the unpolarized case, Melnitchouk, Piller and Thomas [51] derived the most general, antisymmetric, Dirac tensor operator of twist 2 for an off-mass-shell nucleon (see also [52]):

$$\hat{G}^{\mu\nu} = i\epsilon^{\mu\nu\alpha\beta} q_\alpha \left[p_\beta (\not{p}\gamma_5 \hat{G}_p + \not{q}\gamma_5 \hat{G}_q) + \gamma_\beta \gamma_5 \hat{G}_\gamma \right]. \quad (19)$$

Once again, one finds that three functions, \hat{G}_i , can be constructed in terms of scalar and pseudo-scalar vertices. However, in this case there is a new feature, *the function \hat{G}_p does not contribute for a free nucleon*, whereas it does contribute in a nucleus.

The spin-dependent deuteron structure function is given by the trace of $\hat{G}^{\mu\nu}$ with a spin-dependent ND amplitude [51], which can be evaluated using the relativistic DNN vertex of Ref.[24]. Surprisingly, Fig.5 shows that the ratio of the convolution approximation to the fully off-shell calculation (the dashed curve) is even closer to unity in this case than in the spin-independent case.

The comparison between the solid and dotted curves in Fig.5 shows that Eq.(15) is reliable at the 2% level for x below 0.7. However, the excellent agreement in this region between (15) and the full calculation relies on a knowledge of the deuteron D -state probability. As shown in Ref.[51], a change of ω_D by 2% (e.g. from 4% to 6%) leads to an error of order 10% or more in g_1^n . For $x > 0.7$, on the other hand, the approximation (15) fails dramatically. This will be extremely important when testing the predictions of PQCD for the $x \rightarrow 1$ behavior of the polarized distributions in Eqs.(16)–(18).

The use of a polarized ^3He target reduces the errors arising from the extraction, but in that case we have, as yet, no analogue of the relativistic vertex which permitted an

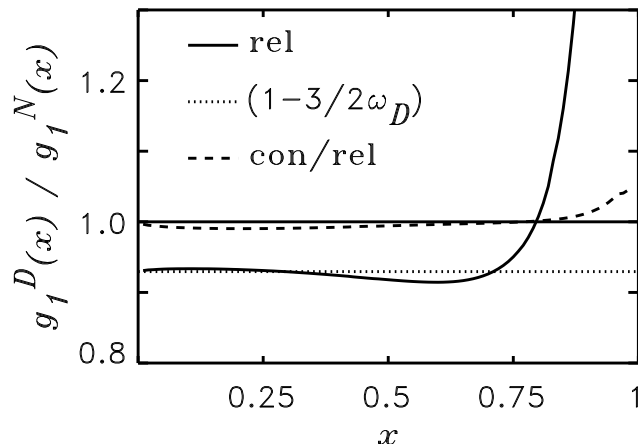


Figure 5. Ratio of deuteron and nucleon structure functions in the full model (solid), and with a constant depolarization factor corresponding to $\omega_D = 4.7\%$ (dotted line). The dashed curve is the ratio of g_1^D calculated via convolution to g_1^D calculated in the relativistic model — from Ref.[51].

estimate of off-shell corrections in the deuteron case. As the binding energy and density of the target nucleus increases we expect these corrections to increase as well. In particular, while the new structure function \hat{G}_p contributes only at order $(v/c)^3$ and is negligible for the deuteron, one cannot yet discount the possibility of \hat{G}_p playing a significant role in nuclei heavier than the deuteron.

3. THE DEUTERON AT SMALL x

At decreasing values of Bjorken- x , as sea quarks begin to dominate, the impulse approximation should eventually break down. One expects that coherent, multiple scattering effects become important when the characteristic time scale, $1/Mx$, of the DIS process becomes larger than the typical average distance between nucleon in the nucleus. This occurs typically in the region $x < 0.1$. Such effects are certainly seen in the low- x depletion of the nuclear EMC ratio in heavy nuclei. Any shadowing in the deuteron should therefore produce a depletion in the ratio F_2^D/F_2^N at small x [53–58].

A deviation from unity of F_2^D/F_2^N at low x is highly relevant for understanding the violation of the Gottfried sum rule, which measures the integrated difference between the proton and neutron structure functions. The violation, discovered by the New Muon Collaboration in 1990 [59], was interpreted as a sizable difference between \bar{d} and \bar{u} in the proton, but relies on an accurate determination of nuclear corrections to F_2^D .

An excess of \bar{d} over \bar{u} cannot be understood in terms of PQCD — it is a property of the “intrinsic sea” of the nucleon. We briefly review the interpretation of this excess,

including the widely accepted explanation in terms of the pion cloud of the nucleon, first suggested in 1983 [8,60]. As the pion cloud of the nucleon is an unavoidable consequence of dynamical symmetry breaking in QCD this experimental discovery offers important insight into the realization of non-perturbative QCD in the structure of the nucleon.

3.1. Nuclear Shadowing

The rescattering of a virtual photon from both nucleons in the deuteron is usually described within the Glauber multiple scattering formalism. Corrections associated with a relativistic deuteron wave function amount to a few percent out of a shadowing correction to F_2^D that is only a few percent in total, and hence can be neglected. At small x , nuclear binding and Fermi motion corrections can be neglected, and the total deuteron structure function written as:

$$F_2^D(x, Q^2) \approx \frac{1}{2} \left(F_2^p(x, Q^2) + F_2^n(x, Q^2) + \delta^{(\text{shad})} F_2^D(x, Q^2) \right). \quad (20)$$

In modeling the shadowing correction, $\delta^{(\text{shad})} F_2^D$, our approach is to take a two-phase model, similar to that of Kwiecinski and Badelek [53–55]. At high virtuality the interaction of the virtual photon with the deuteron is parameterized in terms of diffractive scattering through the double and triple Pomeron, as well as scattering from exchanged mesons in the deuteron. On the other hand, at low virtuality it is most natural to apply a vector meson dominance (VMD) model, in which the virtual photon interacts with the nucleons via its hadronic structure, namely the ρ^0 , ω and ϕ mesons. The latter contribution vanishes at sufficiently high Q^2 , but for $Q^2 < 1 \text{ GeV}^2$ it is, in fact, responsible for the majority of the dependence on Q^2 .

For the diffractive component, Pomeron (IP) exchange between the projectile and both constituent nucleons models the interaction of partons from different nucleons within the deuteron. Assuming factorization of the diffractive cross section, the shadowing correction (per nucleon) to the deuteron structure function from IP -exchange is written as a convolution of the Pomeron structure function, F_2^{IP} , with a distribution function f_{IP} , describing the number density of exchanged Pomerons:

$$\delta^{(IP)} F_2^D(x, Q^2) = \int_{y_{\min}}^2 dy f_{IP}(y) F_2^{IP}(x_{IP}, Q^2), \quad (21)$$

where, treating the deuteron non-relativistically, [53–57]:

$$f_{IP}(y) = -\frac{\sigma_{pp}}{8\pi^2} \frac{1}{y} \int d^2\mathbf{k}_T S_D(\mathbf{k}^2). \quad (22)$$

Here, $y = x(1 + M_X^2/Q^2)$ is the light-cone momentum fraction carried by the Pomeron (M_X is the mass of the diffractive hadronic debris), and $x_{IP} = x/y$ is the momentum fraction of the Pomeron carried by the struck quark in the Pomeron. The deuteron form factor, $S_D(\mathbf{k}^2)$, is given in terms of the coordinate space wave functions:

$$S_D(\mathbf{k}^2) = \int_0^\infty dr |\psi_D(r)|^2 j_0(|\mathbf{k}|r), \quad (23)$$

where j_0 is a spherical Bessel function. Within experimental errors, the factorization hypothesis, as well as the y dependence of $f_{IP}(y)$ [53–57], is consistent with the recent

HERA data [61] obtained from observations of large rapidity gap events in diffractive ep scattering. These data also confirm previous findings that the Pomeron structure function contains both a hard and a soft component: $F_2^{IP}(x_{IP}, Q^2) = F_2^{IP(\text{hard})}(x_{IP}, Q^2) + F_2^{IP(\text{soft})}(x_{IP}, Q^2)$. The hard component of F_2^{IP} is generated from an explicit $q\bar{q}$ component of the Pomeron, and has an x_{IP} dependence given by $x_{IP}(1 - x_{IP})$ [62], in agreement with the recent diffractive data [61]. The soft part, which is driven at small x_{IP} by the triple-Pomeron interaction [53], has an x_{IP} dependence typical of a sea-quark distribution, with normalization fixed by the triple-Pomeron coupling constant.

The dependence of F_2^{IP} on Q^2 [54], at large Q^2 , leads to a weak (logarithmic) Q^2 dependence for the shadowing correction $\delta^{(IP)}F_2^D$. The low- Q^2 extrapolation of the $q\bar{q}$ component is parameterized by applying a factor $Q^2/(Q^2 + Q_0^2)$, where $Q_0^2 \approx 0.485 \text{ GeV}^2$ may be interpreted as the inverse size of partons inside the virtual photon [63]. For the nucleon sea quark densities relevant for $F_2^{IP(\text{soft})}$ we use the recent parametrization of Donnachie and Landshoff, which includes a low- Q^2 limit consistent with the real photon data, in which case the total Pomeron contribution $\delta^{(IP)}F_2^D \rightarrow 0$ as $Q^2 \rightarrow 0$ [63].

An adequate description of shadowing at small Q^2 requires a higher-twist mechanism, such as vector meson dominance. VMD is empirically based on the observation that some aspects of the interaction of photons with hadronic systems resemble purely hadronic interactions. In terms of QCD this is understood in terms of a coupling of the photon to a correlated $q\bar{q}$ pair of low invariant mass, which may be approximated as a virtual vector meson. One can then estimate the amount of shadowing in terms of the multiple scattering of the vector meson using Glauber theory. The corresponding correction (per nucleon) to the nuclear structure function is:

$$\delta^{(V)}F_2^D(x, Q^2) = \frac{Q^2}{\pi} \sum_V \frac{\delta\sigma_{VD}}{f_V^2(1 + Q^2/M_V^2)^2}, \quad (24)$$

where

$$\delta\sigma_{VD} = -\frac{\sigma_{VN}^2}{8\pi^2} \int d^2\mathbf{k}_T S_D(\mathbf{k}^2) \quad (25)$$

is the shadowing correction to the vector meson–nucleus cross section, f_V is the photon–vector meson coupling strength, and M_V is the vector meson mass ($V = \rho^0, \omega, \phi$) are important at low Q^2 . The vector meson propagators in Eq.(24) lead to a strong Q^2 dependence of $\delta^{(V)}F_2^D$, which peaks at $Q^2 \sim 1 \text{ GeV}^2$. For $Q^2 \rightarrow 0$ and fixed x , $\delta^{(V)}F_2^D$ disappears due to the vanishing of the total F_2^D . Furthermore, since this is a higher twist effect, shadowing in the VMD model dies off quite rapidly between $Q^2 \sim 1$ and 10 GeV^2 , so that for $Q^2 > 10 \text{ GeV}^2$ it is almost negligible — leaving only the diffractive term, $\delta^{(IP)}F_2^D$. (Note that at fixed ν , for decreasing Q^2 the ratio F_2^D/F_2^p approaches the photoproduction limit.)

3.2. Meson Exchange Currents

Meson exchange currents (MEC) are familiar in few-body physics. In the context of DIS they have been recognized as a potentially important, many-body correction, which does indeed scale, since the possible enhancement of the nuclear pion field was proposed [64,65] as an explanation of the nuclear EMC effect. In the deuteron case, Kaptari *et*

al. have suggested [66] that MEC may lead to some *antishadowing* corrections to $F_2^D(x)$. The total contribution to the deuteron structure function from meson exchange is:

$$\delta^{(M)} F_2^D(x, Q^2) = \sum_M \int_x dy f_M(y) F_2^M(x/y, Q^2), \quad (26)$$

where $M = \pi, \rho, \omega, \sigma$. The virtual meson structure function, F_2^M , one approximates by the (real) pion structure function, for which data has been obtained through the Drell-Yan process. The exchange-meson distribution functions, $f_M(y)$, are obtained from the non-relativistic reduction of the nucleon-meson interaction given in Refs.[56,66]. In practice pion exchange is the dominant process, and gives a positive contribution to $\delta^{(M)} F_2^D$. The exchange of the fictitious σ meson (which represents correlated 2π exchange) also gives rise to antishadowing for small x . Vector meson exchange cancels some of this antishadowing, however the magnitude of this is smaller. In fact, for not too hard meson-nucleon vertices all contributions other than that of the pion are essentially negligible.

3.3. Neutron Structure Function at Small x

In the region $x < 0.1$ the magnitude of the (negative) Pomeron/VMD shadowing is larger than the (positive) meson-exchange contribution, so that the total $\delta^{(\text{shad})} F_2^D = \delta^{(IP)} F_2^D + \delta^{(V)} F_2^D + \delta^{(M)} F_2^D$ is negative. On the other hand, at slightly larger x (~ 0.1 – 0.2), there is a very small amount of antishadowing, which is due mainly to the VMD and pion-exchange contributions. In the kinematic region covered by NMC, $x > 0.004$, $Q^2 = 4 \text{ GeV}^2$ [67], the overall effect on the shape of the neutron structure function is a 1–2% *increase* in $F_2^n/F_2^{n(\text{bound})}$ for $x < 0.01$, where $F_2^{n(\text{bound})} \equiv F_2^D - F_2^p$.

The presence of shadowing in the deuteron would be confirmed through observation of a deviation from unity in the F_2^D/F_2^p structure function ratio in the kinematic region where Regge theory is expected to be valid. Although the exact value of x below which the proton and (free) neutron structure functions become equivalent is not known, it is expected that at low enough x , $F_2^p \rightarrow F_2^n$, in which case $F_2^D/F_2^p \rightarrow 1 + \delta^{(\text{shad})} F_2^D/2F_2^p$. Subtracting the shadowing correction from the deuteron data should then yield $F_2^p - F_2^n \rightarrow 0$ as $x \rightarrow 0$. While for the lowest NMC data point it may be debatable whether the Regge region is reached, the E665 Collaboration [68] has taken data to very low x , $x \sim 10^{-5}$, which should be much nearer the onset of Regge behavior.

In Fig.6 we show the ratio F_2^n/F_2^p extracted from the low x E665 Collaboration data [68], as well as the earlier NMC data at larger x [67], which have been corrected for the effects of shadowing and MEC [69] (note that the E665 data are not taken at fixed Q^2). With these corrections, the data are in fact consistent with the hypothesis that $F_2^n = F_2^p$ in the small x region (say $x < 10^{-3}$).

3.4. The Gottfried Sum Rule

The main interest in the NMC measurement of the neutron structure function at low x was an accurate test of the Gottfried sum rule:

$$S_G = \int_0^1 dx \frac{F_2^p(x) - F_2^n(x)}{x} \quad (27)$$

$$= \frac{1}{3} - \int_0^1 dx (\bar{d}(x) - \bar{u}(x)). \quad (28)$$

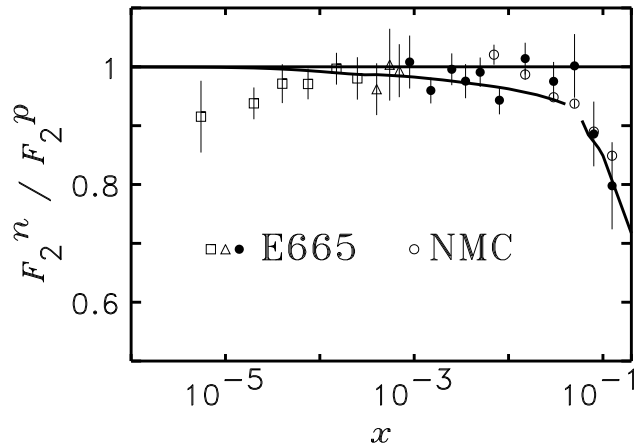


Figure 6. x dependence of the F_2^n/F_2^p structure function ratio, compared with the values extracted from the E665 [68] and NMC data [67], and corrected for nuclear shadowing.

In the naive quark model, where $\bar{d} = \bar{u}$, this gives $S_G = 1/3$. Ignoring nuclear effects, the most recent experimental value obtained by the NMC (over the range 0.004 to 0.8) is $S_G^{\text{exp}} = 0.2281 \pm 0.0065$ [70], indicating a clear violation of SU(2) flavor symmetry in the proton's sea. However, because the structure function difference in S_G is weighted by a factor $1/x$, any small differences between F_2^n and $F_2^{n(\text{bound})}$ are amplified for $x \rightarrow 0$.

Including the nuclear corrections, the overall effect on the experimental value for S_G :

$$S_G = S_G^{\text{exp}} + \int_0^1 dx \frac{\delta^{(\text{shad})} F_2^D(x)}{x}, \quad (29)$$

is a reduction of between -0.010 and -0.026 , or about 4 and 10% of the measured value without the shadowing correction [56]. Therefore a value that reflects the “true” Gottfried sum should be around $S_G \approx 0.2$, which represents some 30% reduction from the naive quark model prediction, $S_G = 1/3$.

3.5. SU(2)_F Violation and the Chiral Structure of the Nucleon

The fundamental degrees of freedom in QCD are quarks and gluons, and for a considerable time there was great reluctance to include any other degrees of freedom in modeling hadron structure. On the other hand, extensive studies of non-perturbative QCD have shown that the chiral symmetry of the QCD Lagrangian is dynamically broken and that the resulting, massive constituent quarks must be coupled to pions. As pseudo-Goldstone bosons, the latter would be massless in the chiral limit. Most importantly, as emphasised by extensive work on chiral perturbation theory, *no perturbative treatment of $q\bar{q}$ creation and annihilation can ever generate the non-analytic behaviour in the light quark mass for physical quantities (such as $M, \langle r^2 \rangle, \sigma_{\pi N}$) which are generated by these Goldstone*

bosons. As a consequence, it is now difficult to imagine a realistic quark model which does not incorporate at least the pion cloud of the nucleon.

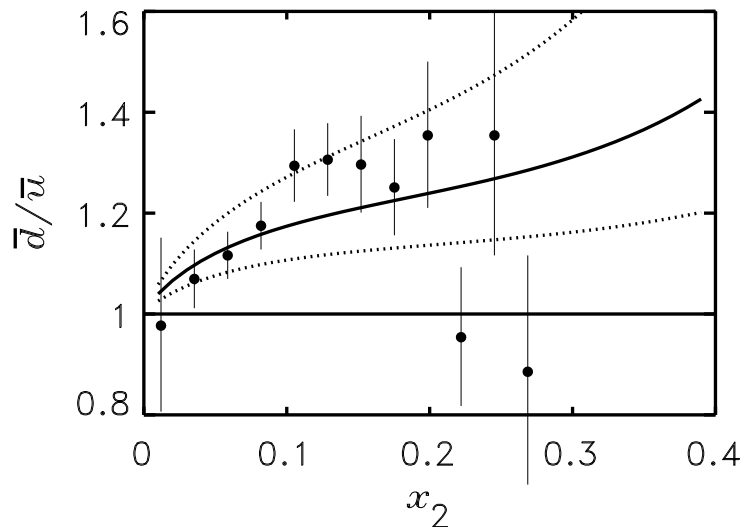


Figure 7. Comparison of the value of \bar{d}/\bar{u} extracted from the recent E866 data [7] with the expectations from just the πN Fock component of the nucleon wave function, for three different form factors at the πN vertex.

The early development of chiral quark models began in the late 1970's [60,71–73] and it became clear that the pion field had very important practical consequences for the low energy properties of hadrons. For example, the coupling to a “bare” nucleon lowers its mass by several hundred MeV, and can contribute a large part of the $N - \Delta$ mass difference, while the charge form factor of the neutron is a first order effect of its pion cloud [60].

However, the relevance of the pion cloud for deep inelastic scattering, which had been first realized by Feynman and Sullivan [74], was not explored in depth until the discovery of the nuclear EMC effect, when it was suggested that the effect might be caused by a nuclear enhancement of the pion field of the bound nucleons [64,65]. At this time it was realized that the light mass of the pion would lead to an enhancement of the non-strange over the strange sea of the nucleon [8], which was used to put a constraint on the pion–nucleon form factor — a limit that has since been explored in detail [75]. A more important consequence of the nucleon’s pion cloud, which was also pointed out in Ref.[8], was an excess of \bar{d} over \bar{u} quarks. In particular, simple Clebsch-Gordan coefficients for isospin show that the pion cloud of the proton is in the ratio 2:1 for $\pi^+ : \pi^0$. Since the π^+ contains only a valence \bar{d} and the π^0 equal amounts of \bar{d} and \bar{u} , this component of the

pion cloud of the nucleon yields a ratio for $\bar{d} : \bar{u}$ of 5:1.

On the other hand, perturbative QCD inevitably leads to the conclusion that $\bar{u} = \bar{d}$, a result known as SU(2)-flavor, SU(2)_F, symmetry. The latter is a very misleading name as there is *no rigorous symmetry involved*. Indeed, the prediction that the component of the sea arising from the long-range piece of the pion cloud of the nucleon satisfies $\bar{d} : \bar{u} = 5:1$ is totally consistent with charge independence. Thus the violation of the Gottfried sum rule and the subsequent measurement of $\bar{d} - \bar{u}$ gives us direct evidence that there is a sizable non-perturbative component of the nucleon sea. Various studies of the pion cloud of the nucleon since the original NMC measurement [6] have concluded that this is indeed the most likely explanation of the observed violation of the sum rule [9,76–79].

In Fig.7 we show the calculated ratio of \bar{d}/\bar{u} from the πN Fock component of the nucleon wave function as a source of asymmetry, in comparison with the data points extracted from the preliminary results [7] from the E866 collaboration on the ratio of pD and pp Drell-Yan cross sections. The calculation was performed in the light-cone formalism [80,81] with a monopole πNN form factor mass parameter $\Lambda = 0.7, 1.0$ and 1.3 GeV — from smallest to largest. Clearly the agreement is qualitatively excellent, but a more detailed analysis needs to be carried out once all the data have been analysed. Let us emphasise once more the importance of these data, which are giving us direct insight into the way dynamical chiral symmetry breaking is realized in the nucleon.

3.6. Other Non-perturbative Components of the Sea

The experience with the breaking of SU(2)_F symmetry which we have just described leads us to take much more seriously the possibility of an intrinsic component of the strange and charm quark sea. The former was first discussed by Signal and Thomas [82] and has recently been investigated by a number of authors [44,83] in the light of new neutrino data from CCFR [84]. This will clearly be the subject of much more detailed investigation in future. With regard to the question of intrinsic charm [44,46], we refer to our earlier discussion of the HERA anomaly for some sense of the issues involved. This too will clearly be a subject of intense investigation over the next few years.

4. CONCLUSION

At this stage it should be clear that the study of deep-inelastic scattering from few-body systems, notably the deuteron, provides a rich source of new information on hadron structure. It is a fascinating source of challenges for few-body physicists, including such issues as relativity, off-shell effects, meson exchange currents and vector meson dominance.

As the result of a careful analysis of binding effects in deep-inelastic scattering from the deuteron, there has been a dramatic change in the experimental value of the d/u ratio in the valence region. It seems to be consistent with the perturbative QCD prediction that $d/u \rightarrow 1/5$ as $x \rightarrow 1$, rather than 0 — as assumed in all standard parton distributions (and text books). This analysis strongly indicates a need for alternative determinations of d/u — e.g. through semi-inclusive measurements — just to be sure. Meanwhile, there is an urgent need to work out the quantitative consequences for this finding in the kinematic region relevant to the HERA anomaly.

It was reassuring that the model dependent analysis of the “non-convolution” corrections in the deuteron gave values of order 1–2%. However, it remains an open question

how big they could be in heavier nuclei. In particular, it would be of great interest to have a relativistic $^3\text{He-N}$ vertex of the Gross type. This is even more important because ^3He is usually used in the determination of g_1^n .

In the small- x region a careful analysis of recent CERN and Fermilab data in terms of VMD, Pomeron and meson exchange corrections suggests that F_2^n and F_2^p are equal below $x \sim 10^{-3}$. A very important discovery in this region has been the violation of the Gottfried sum rule. The physics involved in this violation has been made explicit by recent data from the E866 Collaboration at Fermilab, which shows the x -dependence of the difference between \bar{d} and \bar{u} .

The theoretical origin of the $\bar{d}-\bar{u}$ difference seems to be the pion cloud of the nucleon, which in turn is a direct consequence of dynamical chiral symmetry breaking. Further study of the shape of this component of the intrinsic sea of the nucleon should throw new light on the way chiral symmetry is realized in non-perturbative QCD. From another point of view, the verification of this prediction for the light quark sea leads us to be bolder in looking for differences between s and \bar{s} , and c and \bar{c} .

To conclude, we have seen that deep inelastic scattering is potentially a gold mine of information concerning the structure of hadronic matter. Thus far we have really only begun to scratch the surface.

Acknowledgements

We would like to acknowledge important contributions to the work described here by A. W. Schreiber and G. Piller. This work was supported by the Australian Research Council, and the DOE grant DE-FG02-93ER-40762.

REFERENCES

1. J.J. Aubert *et al.* (EMC), Phys. Lett. B **123** (1983) 275; Nucl. Phys. **B293** (1987) 740.
2. M. Arneodo *et al.*, Phys. Rep. **240** (1994) 301.
3. D.F. Geesaman, K. Saito and A.W. Thomas, Annu. Rev. Nucl. Part. Sci. **45** (1995) 337.
4. P.A.M. Guichon *et al.*, Nucl. Phys. **A601** (1996) 349.
5. K. Saito and A.W. Thomas, Nucl. Phys. **A574** (1994) 659.
6. P. Amaudruz *et al.* (NMC), Phys. Lett. B **295** (1992) 159; Phys. Rev. Lett. **66** (1991) 2712.
7. E.A. Hawker *et al.* (E866 Collaboration), "Measuring the $\bar{u} - \bar{d}$ Asymmetry in the Proton Sea", presented at XXXII Moriond Conference, 22-29 March 1997.
8. A.W. Thomas, Phys. Lett. **126** B (1983) 97.
9. J. Speth and A.W. Thomas, "Mesonic Contributions to the Spin and Flavor Structure of the Nucleon" (Jül-3283, Sept. 1996), to appear in Adv. Nucl. Phys. (1997).
10. D. Kusno and M. Moravcsik, Phys. Rev. D **20** (1979) 2734.
11. W.B. Atwood and G.B. West, Phys. Rev. D **7** (1973) 773.
12. A. Bodek and J.L. Ritchie, Phys. Rev. D **23** (1981) 1070.
13. L.L. Frankfurt and M.I. Strikman, Phys. Lett. B **76** (1978) 333; Phys. Rep. **76** (1981) 215.
14. L.P. Kaptari and A.Yu. Umnikov, Phys. Lett. B **259** (1991) 155.

15. F. Gross and S. Liuti, Phys. Rev. C **45** (1992) 1374;
16. M.A. Braun and M.V. Tokarev, Phys. Lett. B **320** (1994) 381.
17. G.V. Dunne and A.W. Thomas, Nucl. Phys. **A455** (1986) 701.
18. K. Nakano and S.S.M. Wong, Nucl. Phys. **A530** (1991) 555.
19. L.L. Frankfurt and M.I. Strikman, Phys. Rep. **160** (1988) 235.
20. H. Jung and G.A. Miller, Phys. Lett. B **200** (1988) 351.
21. R.L. Jaffe, in *Relativistic Dynamics and Quark-Nuclear Physics*, eds. M.B. Johnson and A. Picklesimer (Wiley, New York, 1985). S.V. Akulinichev, S.A. Kulagin and G.M. Vagradov, Phys. Lett. B **158** (1985) 485; S.A. Kulagin, G. Piller and W. Weise, Phys. Rev. C **50** (1994) 1154.
22. W. Melnitchouk, A.W. Schreiber and A.W. Thomas, Phys. Rev. D **49** (1994) 1183.
23. R. Blankenbecler and L.F. Cook, Phys. Rev. **119** (1960) 1745.
24. W.W. Buck and F. Gross, Phys. Rev. D **20** (1979) 2361; R.G. Arnold, C.E. Carlson and F. Gross, Phys. Rev. C **21** (1980) 1426; F. Gross, J.W. Van Orden and K. Holinde, Phys. Rev. C **45** (1992) 2094.
25. B.D. Kiester and J.A. Tjon, Phys. Rev. C **26** (1982) 578; J.A. Tjon, Nucl. Phys. **A463** (1987) 157C; D. Plumper and M.F. Gari, Z. Phys. A **343** (1992) 343.
26. P. Mulders, A.W. Schreiber and H. Meyer, Nucl. Phys. **A549** (1992) 498.
27. W. Melnitchouk, A.W. Schreiber and A.W. Thomas, Phys. Lett. B **335** (1994) 11.
28. L.W. Whitlow *et al.*, Phys. Lett. B **282** (1992) 475.
29. T. Uchiyama and K. Saito, Phys. Rev. C **38** (1988) 2245.
30. J. Carbonell, B. Desplanques, V.A. Karmanov and J.-F. Mathiot, to appear in Phys. Rep.
31. W. Melnitchouk and A.W. Thomas, Phys. Lett. B **377** (1996) 11.
32. A. Bodek *et al.*, Phys. Rev. D **20** (1979) 1471; A. Bodek and J.L. Ritchie, Phys. Rev. D **23** (1981) 1070.
33. M. Arneodo *et al.* (NMC), Phys. Lett. B **364** (1995) 107.
34. F.E. Close, *An Introduction to Quarks and Partons* (Academic Press, 1979).
35. F.E. Close, Phys. Lett. B **43** (1973) 422.
36. R. Carlitz, Phys. Lett. B **58** (1975) 345.
37. F.E. Close and A.W. Thomas, Phys. Lett. B **212** (1988) 227.
38. G.R. Farrar and D.R. Jackson, Phys. Rev. Lett. **35** (1975) 1416.
39. S.J. Brodsky, M. Burkardt and I. Schmidt, Nucl. Phys. **B441** (1995) 197.
40. J. Gomez *et al.*, Phys. Rev. D **49** (1994) 4348.
41. H. Abramowicz *et al.* (CDHS Collaboration), Z. Phys. C **25** (1983) 29.
42. C. Adloff *et al.* (H1 Collaboration), hep-ex/9702012.
43. J. Breitwig *et al.* (ZEUS Collaboration), hep-ex/9702015.
44. S.J. Brodsky and B.-Q. Ma, Phys. Lett. B **381** (1996) 317.
45. S. Kuhlmann, H.L. Lai and W.-K. Tung, hep-ph/9704338.
46. W. Melnitchouk and A.W. Thomas, hep-ph/9707387.
47. H.-Y. Cheng, Int. J. Mod. Phys. A **11** (1996) 5109; M. Anselmino *et al.*, Phys. Rep. **261** (1995) 1.
48. J. Ashman *et al.* (EMC), Phys. Lett. B **206** (1988) 364.
49. S.A. Larin, T. van Ritbergen and J.A.M. Vermaseren, hep-ph/9702435.
50. D. Adams *et al.* (SMC), Phys. Lett. B **357** (1995) 248; K. Abe *et al.* (E143 Collabo-

- ration), Phys. Rev. Lett. **75** (1995) 25.
51. W. Melnitchouk, G. Piller and A.W. Thomas, Phys. Lett. B **346** (1995) 165; G. Piller, W. Melnitchouk and A.W. Thomas, Phys. Rev. C **54** (1996) 894.
 52. S.A. Kulagin, W. Melnitchouk, G. Piller and W. Weise, Phys. Rev. C **52** (1995) 932.
 53. J. Kwiecinski and B. Badelek, Phys. Lett. B **208** (1988) 508.
 54. J. Kwiecinski, Z. Phys. C **45** (1990) 461.
 55. B. Badelek and J. Kwiecinski, Nucl. Phys. **B370** (1992) 278; Phys. Rev. D **50** (1994) 4.
 56. W. Melnitchouk and A.W. Thomas, Phys. Rev. D **47** (1993) 3783.
 57. W. Melnitchouk and A.W. Thomas, Phys. Lett. B **317** (1993) 437.
 58. V.R. Zoller, Z. Phys. C **54** (1992) 425; G. Piller, W. Ratzka and W. Weise, Z. Phys. A **352** (1995) 427; H. Khan and P. Hoodbhoy, Phys. Lett. B **298** (1993) 181.
 59. P. Amandruz *et al.* (NMC), Phys. Rev. Lett. **66** (1991) 2712.
 60. S. Th  berge, G.A. Miller and A.W. Thomas, Phys. Rev. D **22** (1980) 2838; *ibid* D **23** (1981) 2106(e); A.W. Thomas, Adv. Nucl. Phys. **13** (1984) 1; G.A. Miller, Int. Rev. Nucl. Phys. **2** (1984) 190.
 61. T. Ahmed *et al.*, Phys. Lett. B **348** (1995) 681.
 62. A. Donnachie and P.V. Landshoff, Phys. Lett. B **191** (1987) 309.
 63. A. Donnachie and P.V. Landshoff, Z. Phys. C **61** (1994) 139.
 64. C.H. Llewellyn Smith, Phys. Lett. B **128** (1983) 107.
 65. M. Ericson and A.W. Thomas, Phys. Lett. B **128** (1983) 112.
 66. L.P. Kaptari, A.I. Titov, E.L. Bratkovskaya and A.Yu. Umnikov, Nucl. Phys. **A512** (1990) 684.
 67. M. Arneodo *et al.* (NMC), Phys. Rev. D **50** (1994) 1.
 68. M.R. Adams *et al.* (E665 Collaboration), Phys. Rev. Lett. **75** (1995) 1466; Phys. Lett. B **309** (1993) 477.
 69. W. Melnitchouk and A.W. Thomas, Phys. Rev. C **52** (1995) 3373.
 70. E. Kabuss (NMC), hep-ph/9706435.
 71. T. Inoue and T. Maskawa, Prog. Theor. Phys. **54** (1975) 1833.
 72. A. Chodos and C.B. Thorn, Phys. Rev. D **12** (1975) 359.
 73. G.E. Brown and M. Rho, Phys. Lett. B **82** (1979) 177.
 74. J.D. Sullivan, Phys. Rev. D **5** (1972) 1732.
 75. L.L. Frankfurt, L. Mankiewicz and M.I. Strikman, Zeit. Phys. A **334** (1989) 334; W. Koepf, L.L. Frankfurt and M.I. Strikman, Phys. Rev. D **53** (1996) 2586.
 76. E.M. Henley and G.A. Miller, Phys. Lett. B **251** (1990) 453.
 77. A.I. Signal, A.W. Schreiber and A.W. Thomas, Mod. Phys. Lett. A **6** (1991) 271.
 78. S. Kumano and J.T. Londergan, Phys. Rev. D **44** (1991) 717; S. Kumano, hep-ph/9702367.
 79. W.-Y.P. Hwang, J. Speth and G.E. Brown, Zeit. Phys. A **339** (1991) 383.
 80. W. Melnitchouk and A.W. Thomas, Phys. Rev. D **47** (1993) 3794.
 81. V.R. Zoller, Z. Phys. C **60** (1993) 141.
 82. A.I. Signal and A.W. Thomas, Phys. Lett. B **191** (1987) 205.
 83. X. Ji and J. Tang, Phys. Lett. B **362** (1995) 182; H. Holtmann *et al.*, Nucl. Phys. **A569** (1996) 631; W. Melnitchouk and M. Malheiro, Phys. Rev. C **55** (1997) 431.
 84. A. Bazarko *et al.* (CCFR Collaboration), Zeit. Phys. C **65** (1995) 189.